Clam Shell Analysis Using Rational Wavelet Transform

Fred Nicolier, Marc Toubin, Alexandre Baussard, Fred Truchetet
Le2i, 12, rue de la fonderie, 71200 Le Creusot, FRANCE
nicolier@u-bourgogne.fr

Keywords: rational scale factor, wavelet transform, multiresolution analysis, clam shell

Abstract

Wavelets have been widely used for spectral analysis. The dyadic multiresolution analysis (MRA) extends their properties to provide extraction and location of the frequencies composing the signal. We introduce a rational scale factor between two level of decomposition to compute finer analysis. This paper describes a method to construct a MRA based on the rational wavelet transform. This process has been applied to enhance growth increments of a clam shell.

1. INTRODUCTION

Multiresolution analysis (MRA) using the wavelet transform has been a powerful tool to span the information contained in a signal or an image. The multiresolution aspect combined with the interesting spatial and frequency properties of the wavelet transform allow extraction of multiple level of details. Various applications use these features to extract and to locate the main frequencies composing the signal. The spectral accuracy depends on the resolution between two scales of decomposition. The resolution is defined by the scale factor that controls the fineness of the analyse throughout the multiresolution process. The ultimate goal of this research is to develop a method to construct a MRA based on the wavelet transform with a rational scale factor. This rational factor is chosen to fit the signal and therefore it provides a better spectral analysis.

The dyadic MRA was first introduced by Mallat[1] with a scale factor value of 2. In certain cases, this parameter is not close enough to the signal to provide a good analysis. Feauveau[2] refined the scale factor in his quincunx algorithm. He described a non-separable MRA based on a quincunx wavelet transform. Two consecutive sublevels of decomposition are separated by a value of $\sqrt{2}$ as factor of resolution. This two processes are not based on general algorithms allowing a free choice of the scale factor. Blu[3,4] developed a rational extension of the filter banks theory.[5] The rate between two successive scales is a rational number but the main drawback of this method is that it cannot leads to true wavelet analysis.

Our work is inspired by the work of Ausher.[6] He has introduced a formalized definition of the rational MRA and a method to construct the wavelet bases associated.

Aside from being of theoretical interest, a rational MRA has practical applications since it performs finer analysis. An example from earth sciences illustrates the benefit of the rational algorithm in order to process the ecological information enclosed in the outer layer of a freshwater clam.[7] A range image of a clam shell is created from a 3D laser scanning system. The information to be extracted is typically multiscalar i.e. the surface presents low scale and high scale geometrical variations due to growth increments related to climatic and environmental event. The rational MRA is applied to the range image to characterize the clam surface. Comparisons with the dyadic algorithm show that finer results are obtained with the rational process.

The outline of the paper is as follows. The rational pyramidal algorithm that supports the MRA is presented in the first section. This is followed by a construction of Littlewood-Paley's filters for the rational wavelet transform. In the last section this method is illustrated by the determination of growth increments from a bivalve Unio sp and the emphasis is on the comparison of the rational algorithm versus the dyadic one.

2. RATIONAL PYRAMIDAL ALGORITHM

The rational algorithm is formally defined by Ausher as a sequence of embedded subspaces V_j. This definition generalized the MRA concept introduced by Mallat.[1] The scale factor between two consecutive scale rates becomes a rational number.

2.1. Definition

Theorem 1: Let M be a rational real number ($M = \frac{p}{q}, M > 1$). A sequence $\{V_j\}_{j\in\mathbb{Z}}$ of closed subspaces of $L^2(\mathbb{R})$ is a rational multiresolution analysis if the following properties are satisfied

$$\begin{array}{l}\forall j \in \mathbb{Z}, V_{j+1} \subset V_j, \\ \overline{\bigcup_{j\in\mathbb{Z}} V_j} = L^2(\mathbb{R}), \\ \bigcap_{j\in\mathbb{Z}} V_j = \{0\}, \\ \forall j \in \mathbb{Z}, f(x) \in V_j \Leftrightarrow f(M^{-1}x) \in V_{j+1}, \\ \forall k \in \mathbb{Z}, f(x) \in V_0 \Leftrightarrow f(x-k) \in V_0.\end{array}$$

An orthogonal basis of V_j is constructed by dilating and translating a mother function $\varphi(x) \in L^2(\mathbb{R})$. The basis function of V_j (called scaling function) are given as

$$\varphi_{j,n}(x) = M^{-j/2}\varphi(M^{-j}x - n), n \in \mathbb{Z}. \quad (1)$$

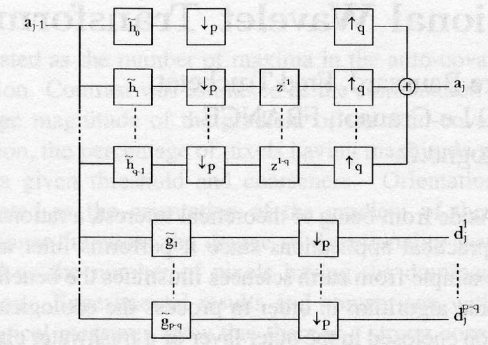

Figure 1. analysis algorithm, decomposition of a discrete approximation a_{j-1} with a rational dilatation factor $M = \frac{p}{q}$.

The orthogonal projection of a function f over V_j is considered as the action of a linear operator A_j on f. Approximation coefficients $a_{j,n}$ of the projection are determined as

$$A_j f = \sum_n \langle f, \varphi_{j,n} \rangle \varphi_{j,n} = \sum_n a_{j,n} \varphi_{j,n}. \quad (2)$$

The orthogonal complement W_j of V_j in V_{j-1} such that $V_{j-1} = V_j \oplus W_j$ is generated by the basis function $\psi_{j,n}(x)$ (wavelets):

$$\psi^m_{j,n}(x) = M^{-\frac{j}{2}} \psi^m(M^{-j}x - nq), \; j, n, m \in \mathbb{Z}. \quad (3)$$

There is $p - q$ wavelets $\psi^1, ..., \psi^{p-q}$ in W_0 constructing an orthonormal basis for $L^2(\mathbb{R})$ and leading to $p - q$ mother wavelets, each generating a subspace W^m_j including in $V_{j-1}(W_j = \bigcup_m W^m_j)$. The linear operator D^m_j over W^m_j is given as $A_{j-1} f = A_j f + \sum_{m=1}^{p-q} D^m_j f$ and detail coefficients are defined by the following relation:

$$D^m_j f = \sum_n \langle f, \psi^m_{j,n} \rangle \psi_{j,n} = \sum_n d^m_{j,n} \psi_{j,n}. \quad (4)$$

2.2. Algorithm

This section gives the basic structure to perform a rational MRA. Both the analysis and synthesis part of the algorithm are described.

Notation: A $p-$upsampler is defined by inserting $(p-1)$ zeros between each sample of the signal. A $q-$downsampler is defined by keeping one sample out of q.

2.2.1. Pyramidal analysis algorithm

The incoming digital signal is taken as the approximation at a given scale because the continuous signal f is hardly available to carry out the analysis The following algorithm computes from an approximation at level $j-1$ the coarser (a_j) and the detail $(d^1_j$ to $d^{p-q}_j)$ coefficients.

From equation (1), the scaling functions $\varphi_{j,n}(x)$ can be written as

$$\varphi_{j,n}(x) = \sum_k h_i[k] \varphi_{j-1, M*(n-i)+k}(x), \quad \text{with } i \text{ such that } M*(n-i) \in \mathbb{Z}, \quad (5)$$

where $h_i[n] = \langle \varphi_{0,-i}, \varphi_{-1,n} \rangle$ represents the impulse response of a numerical filter. The approximation coefficients are expressed from equation (2) and (5): $a_{j,n} = \sum_k h_i[k] \langle f, \varphi_{j-1, M*(n-i)+k} \rangle$. Let $r = M*(n-i)+k$ and $\tilde{h}[n] = h[-n]$,this leads to:

$$a_{j,sq+i} = \sum_r \tilde{h}_i[ps - r] a_{j-1,r} \quad \text{with } s \in \mathbb{Z} \text{ and } i = 0, ..., q-1 \in \mathbb{Z}. \quad (6)$$

Equation (6) shows that the input signal a_{j-1} is first convolved with the filters $\left\{\tilde{h}_i\right\}_{0 \le i \le q-1}$ and one sample out of p is then kept. The output of the downsamplers are delayed by i samples and $q-$upsampled. A final summation of the q signals lead to the coefficients a_j.

The decomposition of the wavelets function $\psi^m(x)$ over V_{-1} is given as

$$\psi^m_{j,n}(x) = \sum_k g^m[k] \varphi_{j-1, np+k}(x) \quad (7)$$

where $g^m[n] = \langle \psi_{0,0}, \varphi_{-1,n} \rangle$. Let $r = np + k$, from equation (4) and (7) it follows:

$$d^m_{j,n} = \sum_r \tilde{g}^m[np - r] a_{j-1,r}. \quad (8)$$

Equation (8) shows that the detail coefficients $d^m_{j,n}$ are computed by first convolving a_{j-1} with the filter $\tilde{g}^m$. One sample out of p is then kept.

The analysis algorithm is constructed from both equation (6) and (8) . The block diagram in Fig. 1 illustrates the structure of the analysis algorithm.

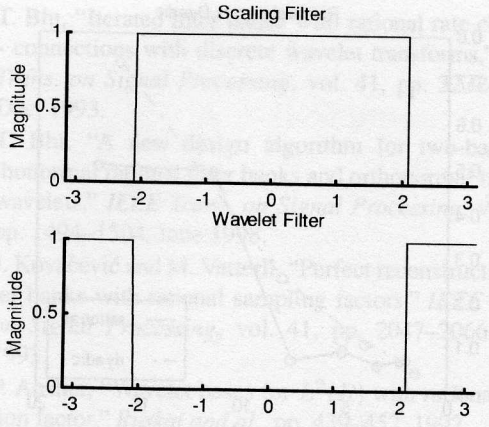

Figure 2. Littlewood-Paley rational filters features for a scale factor $M = \frac{3}{2}$.

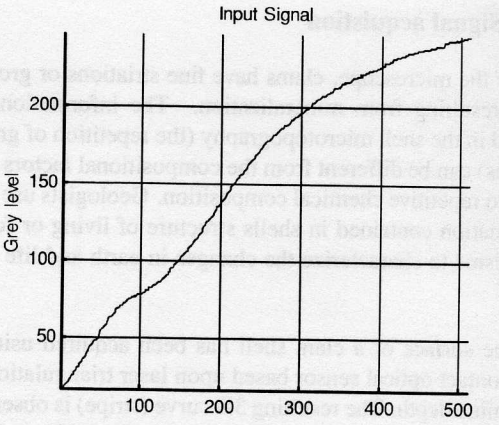

Figure 3. structure of a clam shell. The stripe is 4 cm width with a resolution of 50 μ. The number of samples describing the curve is 516.

2.2.2. Pyramidal synthesis algorithm

The synthesis algorithm can be computed from the analysis equation $A_{j-1}f = \sum_n a_{j,n}\varphi_{j,n} + \sum_m \sum_n d^m_{j,n}\psi^m_{j,n}$. The signal coefficient are reconstructed by summing two signals. They are calculated as:

$$a_{j-1,n} = \sum_k a_{j,k}h_i[n - M*(k-i)] + \sum_m \sum_k d^m_{j,k}g^m[n-kp]. \quad (9)$$

One can notice that if $M = 2$ Mallat's algorithm is recovered.

3. RATIONAL FILTERS

The design of filters for a rational transformation has been studied. This section describes their construction for Littlewood-Paley analysis. There are another base that leads to rational MRA developed by Ausher in.[6]

3.1. Littlewood-Paley

Our goal is to provide a spectral analysis of the clam shell surface. The MRA based on Littlewood-Paley functions is considered as the dual analysis of Haar. They allow fine frequencies analysis.

In the dyadic case ($M = 2$) scaling function and wavelet are defined as

$$\mid \hat{\varphi}(\omega) \mid = 1 \text{ for } -\pi \leq \omega < \pi,$$
$$\mid \hat{\varphi}(\omega) \mid = 0 \text{ for } \pi \leq \omega,$$
$$\hat{\psi}(\omega) = -e^{-i\omega} \text{ for } \pi \leq \mid \omega \mid < \pi,$$
$$\hat{\psi}(\omega) = 0.$$

In the rational case with $M = \frac{p}{q}$ for $m = 1, ..., p-q$, the wavelet is chosen as

$$\hat{\psi}^m(M\omega) = 1 \text{ for } (q+m-1)\tfrac{\pi}{p} \leq \mid \omega \mid < (q+m)\tfrac{\pi}{p},$$
$$\hat{\psi}(\omega) = 0.$$

3.2. Construction

For $M = \frac{3}{2}$, two filters h_i and one filter g are required for the pyramidal algorithm. The coefficients are given by the following relations: $h_i[n] = \langle \varphi_{0,i}, \varphi_{-1,n} \rangle$ and $g[n] = \langle \psi, \varphi_{-1,n} \rangle$. The computation of the filters are performed in Fourier space since their impulsional responses are infinite:

$$\hat{h}_i(\omega) = \sqrt{M}\frac{\hat{\varphi}(M\omega)}{\hat{\varphi}(\omega)}e^{-iM\omega},$$
$$\hat{g}(\omega) = \sqrt{M}\frac{\hat{\psi}(M\omega)}{\hat{\varphi}(\omega)}. \quad (10)$$

Their spectral bandwidth depends on the choice of p and q. Fig. 2 shows the magnitude of Littlewood-Paley's scaling and wavelet filters in Fourier space for a rational scale factor $M = \frac{3}{2}$.

4. CLAM SHELL TOPOGRAPHY

The improvement of the rational analysis versus the dyadic is presented in this section. The comparisons are based on a practical application: a MRA of a clam shell topography in order to extract the frequencies contained at multiple scales.

4.1. Signal acquistion

Under the microscope, clams have fine striations or growth lines resulting from mineralization. The information included in the shell microtopography (the repetition of growth lines) can be different from the compositional factors that refer to repetitive chemical composition. Geologists use this information contained in shells structure of living or fossil organisms to characterize the changes in earth and life history.[?]

The surface of a clam shell has been acquired using a non-contact optical sensor based upon laser triangulation to determine depth. The resulting 3D curve (stripe) is observed through two calibrated CCD cameras, and the 3D position of the stripe points are computed by triangulation. The two cameras are set so that the image of the stripe intersects each image row (or column) once and the range information can be linked directly to one image coordinate. Each row composing the range image are processed separatly as the input of one dimensional signal. Spatial sampling resolution is set in order to have the best match between the scale grid imposed by the use of the rational algorithm and the frequencies to be revealed. Fig. 3 represents an example a scan clam area.

4.2. Rational versus dyadic

Both the dyadic and the rational pyramidal analysis algorithm are performed on the signal. The scaling and wavelet functions are constructed with Littlewood-Paley's bases. The value of the rational scale factor is taken as $M = \frac{3}{2}$. We propose a method to measure the fineness of each MRA. The process consists in computing an energy factor for each details space. The energy factor at a resolution j is defined as

$$E_j = \frac{1}{N_j} \sum_{n=1}^{N_j} (d_{j,n})^2 ,$$

where N_j represents the number of detail coefficients. The normalization parameter N_j allows comparisons between various analysis.

The process is achieved for both dyadic and rational MRA. Resulting curves are reported on the same graphic and an example illustrates this method in Fig. 4. They enhance the fact that the dyadic analysis cannot cover as much scales as the rational analysis.

The generalization of the dyadic algorithm to the rational analysis is based on a rational scale factor. This parameter allows various choices for selecting the analysis scale. The rational scale factor is then designed to be closer to the signal components throughout the multiresolution process.

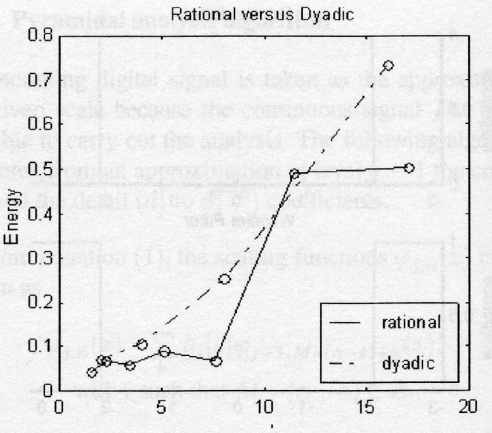

Figure 4. comparisons between the rational and the dyadic MRA: the energy factor is computed for each scale $s = M^j$.

4.3. Clam shell structure

Three major increments has been extracted from the rational MRA. Due to the infinite response of the filters used for the rational MRA, the temporal properties of the bases functions cannot lead to accurate localization of these increments. Further studies are in progress to characterize new bases with better localization features.

5. SUMMARY

The rational MRA extends the potentialities of the dyadic MRA providing a better adaptation of the scale factor to the signal components. The rational pyramidal algorithm and the construction of the Littlewood-Paley filters for rational MRA has been introduced. This method has been illustrated by the measure of growth increments repetition on shell surface in order to determine the various time lags involved in clam biomineralization. The rational multiscale decomposition performed a finer analysis than the dyadic analysis and allows distinction between environmental stress features and growth increments related to bivalve ontogenis. We focus now our researches on the computation of new bases functions with better spatial and temporal features. The multidimensional aspect of the rational MRA is also currently studied.

REFERENCES

1. S. G. Mallat, "A theory for multiresolution signal decomposition : The wavelet representation," *IEEE Trans. on PAMI*, vol. 11, pp. 674–693, July 1989.
2. J.-C. Feauveau, "Analyse multirésolution avec un facteur de résolution $\sqrt{2}$," *Journal de Traitement du Signal*, vol. 7, no. 2, pp. 117–128, 1990.

3. T. Blu, "Iterated filter banks with rational rate changes - connections with discrete wavelet transforms," *IEEE Trans. on Signal Processing*, vol. 41, pp. 3232–3244, Dec. 1993.
4. T. Blu, "A new design algorithm for two-band orthonormal rational filter banks and orthonormal rational wavelets," *IEEE Trans. on Signal Processing*, vol. 46, pp. 1494–1504, June 1998.
5. J. Kovačević and M. Vetterli, "Perfect reconstruction filter banks with rational sampling factors," *IEEE Trans. on Signal Processing*, vol. 41, pp. 2047–2066, June 1993.
6. P. Ausher, "Wavelet bases for $L^2(R)$ with rational dilation factor," *Ruskai and al.*, pp. 439–452, 1992.
7. M. Toubin, O. Laligant, A. Diou, F. Truchetet, E. P. Verrecchia, C. Dumont, and M. A. Abidi, "Multi-scale analysis of shell growth increments using wavelet transform," *Computers and Geosciences, Journal of the International Association for Mathematical Geology*, vol. 25, pp. 877–885, 1999.